

A perturbed utility route choice model*

Mogens Fosgerau[†] Mads Paulsen[‡] Thomas Kjær Rasmussen[§]

December 24, 2024

Abstract

We propose a model in which a utility maximizing traveler assigns flow across an entire network under a flow conservation constraint. Substitution between routes depends on how much they overlap. This model can be estimated from route choice data, where the full set of route alternatives is included and no choice set generation is required. Nevertheless, estimation requires only linear regression and is very fast. Predictions from the model can be computed using convex optimization and is straightforward even for large networks.

Keywords: Route choice; perturbed utility; discrete choice; networks

1 Introduction

Big data is now widely available that traces individual vehicles through complex traffic networks. This opens new possibilities for estimating route choice models that better reflect actual behavior. However, route choice models face the curse of dimensionality, as the number of potential routes through a realistically sized network is extremely large.

This paper formulates a route choice model as a perturbed utility model (Fosgerau and McFadden, 2012; Fudenberg et al., 2015), in which a rational, utility maximizing traveler chooses a network flow that maximizes a concave utility function. Perturbed utility models are firmly rooted in modern microeconomic theory and can be interpreted as representing a population of agents whose individual behavior is described by one of a wide range of discrete choice models, where the additive random utility model is an example. Alternatively, a perturbed utility model can be interpreted at face value to represent the behavior of individual agents who randomize across options (Allen and Rehbeck, 2019).

The first-order conditions for the traveler’s perturbed utility maximization problem are used to formulate a linear regression equation, which allows the parameters of the route choice model to

*This research is funded by the European Research Council (ERC) under the European Union’s Horizon 2020 research and innovation programme (grant agreement No. 740369). We thank Michel Bierlaire, Emma Frejinger and Nikolas Geroliminis for very useful comments.

[†]University of Copenhagen; mogens.fosgerau@econ.ku.dk.

[‡]Technical University of Denmark; madsp@dtu.dk.

[§]Technical University of Denmark; tkra@dtu.dk.

be estimated from observed data. We present a transformation that eliminates the flow conservation constraint such that ordinary least squares estimation is applicable. This is a major step forward, as the simplicity of linear regression allows realistic networks to be handled at low computational cost. In this paper, we formulate the model, analyze its properties, derive an estimator, and then apply the model to simulated and real data with satisfactory results.

We add to a long line of research into route choice models. Early route choice models have relied on maximum likelihood estimation of an additive random utility discrete choice model (McFadden, 1981) for the choice between alternative routes. However, the number of possible routes in a large network is extremely large, comparable to the number of atoms in the universe, even if loops are ruled out. So the main problem for these models is that the number of potential routes is prohibitively large. Much attention has been given to the generation of choice sets with good coverage to avoid bias resulting from excluding relevant alternatives. Similarly, much attention has been given to find models that lead to realistic substitution patterns when alternatives routes overlap more or less.¹ The perturbed utility route choice model operates at the network level and does not require a choice set as input. On the contrary, the perturbed utility route choice model predicts which links are active and the set of routes using these links can be thought of as a consideration set.

Another issue with additive random utility discrete choice models of route choice is that error terms are generally assumed to have full support such that every alternative is chosen with positive probability. This is not necessarily realistic nor desirable in assignment as most feasible routes in a large network are quite nonsensical (Watling et al., 2015, 2018). In contrast, the perturbed utility route choice model predicts real zeros and the number of active routes depends on parameters.

A stream of research has considered recursive models in which the traveler is seen as choosing a path link by link in a Markovian fashion. Earlier papers considered assignment (Dial, 1971; Bell, 1995; Shen et al., 1996; Baillon and Cominetti, 2008). A recent series of papers has considered estimation by maximum likelihood of what they term the recursive logit model and the nested recursive logit model (Fosgerau et al., 2013; Mai et al., 2015a,b). In contrast, estimation of the perturbed utility route choice model does not require computationally demanding maximization of a likelihood function. Where the basic recursive logit model has the IIA property at the route choice level, the perturbed utility route choice model predicts realistic substitution patterns that derive directly from the network structure.

Oyama et al. (2020) cast the assignment problem for the network generalized extreme value model as a concave maximization problem of the perturbed utility form, where the perturbation function is a generalized entropy that incorporates the network structure. This is an instance of the general result that any additive random utility model can be represented as a perturbed utility model (Hofbauer and Sandholm, 2002). In contrast to Oyama et al. (2020), we here consider estimation of the model parameters. We use a perturbation function that allows corner solutions, which avoids assigning positive probability to all routes that are physically possible.

¹Prato (2009) provides a review. A more recent overview of the literature may be found in Oyama et al. (2020).

We set up the model in Section 2 and derive a linear regression equation that can be estimated by ordinary least squares regression. We find the model implies that routes are substitutes and more so the more they overlap. In Section 3 we illustrate the model’s predictions using first a toy network and then a large scale network covering the Copenhagen metropolitan area. In Section 4, we demonstrate that true parameters can be recovered from realistic simulated data from a large network. We go on in Section 5 to estimate the model using a large dataset of GPS traces for trips in the Copenhagen network. We validate the model’s prediction against our data. Section 6 concludes.

2 Setup

A network $(\mathcal{V}, \mathcal{E})$ is defined by an incidence matrix A , which has a row for each vertex (node) $v \in \mathcal{V}$ and a column for each edge (link) $e \in \mathcal{E}$. As we are considering traffic networks, we will talk about links and nodes. The entries of A are $a_{ve} = -1$ if edge/link e leads out of vertex/node v , $a_{ve} = 1$ if link e leads into node v , and $a_{ve} = 0$ otherwise.

A traveler has unit demand given by the vector b , which is a column vector across nodes with -1 at the origin node, 1 at the destination node and zeros otherwise. There is a traveler for each demand vector b , we suppress the dependence on b in the notation.

The columns of A as well as b sum to zero. Therefore let both omit one row, such that we may assume that A has full rank and hence that AA^\top is invertible.

The traveler chooses a non-negative column vector of link flows $x = (x_e)_{e \in \mathcal{E}}$, satisfying flow conservation $Ax = b$ to maximize the concave perturbed utility function

$$\begin{aligned} U(x) &= l^\top (u \circ x) - l^\top F(x) \\ &= l^\top (u \circ x) - l^\top ((1+x) \circ \ln(1+x) - x). \end{aligned} \quad (1)$$

Let us go through the terms in the utility function. Vector $u = (u_e)_{e \in \mathcal{E}}$ has a component for each link and expresses the utility per distance unit of using that link. We assume that all components of u are negative. Vector $l = (l_e)_{e \in \mathcal{E}}$ comprises the link lengths. The term $u \circ x = (u_e x_e)_{e \in \mathcal{E}}$ is the component-wise product of the vector of link utilities and the flow vector. Hence, the term $l^\top (u \circ x)$ is the sum across links of the utility taking length into account, multiplied by the flow.

The second term is the sum across links, weighted by link length, of $F(x) = (F(x_e))_{e \in \mathcal{E}}$, the function F applied component-wise to the flow vector. The crucial properties of F are that it is strictly convex, $F(0) = 0$ and $F'(0) = 0$. The combined function $l^\top F(x)$ is then strictly convex, which rewards the (representative) traveler for diversification and ensures that the utility maximizing flow exists uniquely. At the same time, it is zero and flat at zero flow, which, together with the condition that link utilities are negative, ensures that the optimal flow on any link is zero if the flow conservation constraint is not active there.

The utility function (1) is thus separable as a sum of independent terms across links. The flow

conservation constraint creates dependencies whereby changes in utilities on some links induces changes in flow on other links.

In (1), we specify $F(x_e) = ((1 + x_e) \ln(1 + x_e) - x_e)$, which satisfies the conditions that we have imposed. The specification inherits its general behavioral justification from the perturbed utility (1) and does well in our simulations, but there are many other possible specifications with similar properties.

A notable feature of the model construction is that it is invariant to link splitting. Consider a link e with a contribution to the utility that is $l_e u_e x_e - l_e F(x_e)$, and split that link into two links e_1, e_2 with $l_e = l_{e_1} + l_{e_2}$, $x_e = x_{e_1} = x_{e_2}$ and $u_e = u_{e_1} = u_{e_2}$. Then

$$l_e u_e x_e - l_e F(x_e) = l_{e_1} u_{e_1} x_{e_1} - l_{e_1} F(x_{e_1}) + l_{e_2} u_{e_2} x_{e_2} - l_{e_2} F(x_{e_2}).$$

In other words, the utility contribution of the whole link is equal to the sum of the contributions of the two parts. This is a desirable model feature as it makes the predictions of the model invariant with respect to the introduction of dummy nodes.

The utility vector u is specified as a linear function $u = z\beta$ of link characteristics organized in a matrix z and parameters organized in a column vector β to be estimated.

Even though the utility function (1) does not comprise an explicit representation of heterogeneity, it may still be interpreted as representing an underlying heterogeneous population of travelers.

2.1 Solving the traveler's problem

The Lagrangian for the traveler's problem is

$$\Lambda(x, \lambda) = l^\top (u \circ x) - l^\top ((1 + x) \circ \ln(1 + x) - x) + \lambda^\top (Ax - b),$$

where $\lambda \in \mathbb{R}^{|\mathcal{V}|-1}$ is a vector of Lagrange multipliers, one for each node in the network (less one), corresponding to the flow conservation constraints. For each link e , x_e is either 0 or the partial derivative of the Lagrangian with respect to x_e is zero. Altogether we have the first-order conditions

$$\begin{aligned} 0 &= \hat{x} \circ \left(l \circ (u - \ln(1 + \hat{x})) + A^\top \hat{\lambda} \right) \\ A\hat{x} &= b, \end{aligned}$$

where hats denote optimal values of x and λ .

We can give the first-order condition an intuitive interpretation, noting that for links with positive flow, the marginal utilities $u_e - \ln(1 + x_e)$ are equal, except for the effect induced by the flow conservation constraint.

Let B be a matrix that is the $|\mathcal{E}|$ -dimensional identity matrix, except (at least) all rows corresponding to edges with zero flows are omitted. Pre-multiplying the first-order condition by B , we can disregard links with zero flows (and possibly more), obtaining

$$B(l \circ u) = B(l \circ \ln(1 + \hat{x})) - BA^\top \hat{\lambda}. \quad (2)$$

We allow that B omits also rows corresponding to some positive flows. This can be useful when we work with flow data constructed from vehicle trajectories as it accommodates the possibility that we omit rows corresponding to links with small vehicle counts. We have not made use of this possibility in the results presented in this paper.

Equation (2) can be used to formulate a regression model. For each origin-destination pair, the corresponding traveler's problem leads to vectors $(\hat{x}, \hat{\lambda})$ where the elements of $B(l \circ \ln(1 + \hat{x}))$ can be used as dependent variables.

Noting that

$$B(l \circ u) = B(l \circ z\beta) = B(l \circ z)\beta,$$

the matrix $B(l \circ z)$ can act as independent variables with corresponding parameter vector β . The Lagrange multipliers $\hat{\lambda}$ can be treated as fixed effects, that can be corrected for in the regression. That is, however, computationally challenging, as $\hat{\lambda}$ has the size equal to the number of nodes in the network and the vector is specific to each origin-destination combination. The number of fixed effects may therefore become very large as the size of the network and the number of origin-destination combinations grows. We will therefore seek an alternative regression equation that eliminates $\hat{\lambda}$.

2.2 Eliminating the Lagrange multipliers

Let $C = (BA^\top)^*$ be a Moore-Penrose inverse of BA^\top . We may then utilize that $BA^\top CBA^\top = BA^\top$. Multiplying the traveler's reduced first-order condition (2) by $BA^\top C$, we find that

$$\begin{aligned} BA^\top CB(l \circ u) &= BA^\top CB(l \circ \ln(1 + x)) - BA^\top CBA^\top \lambda \\ &= BA^\top CB(l \circ \ln(1 + x)) - BA^\top \lambda, \end{aligned}$$

which leads to

$$BA^\top \lambda = BA^\top CB(l \circ (\ln(1 + x) - u)).$$

Plugging this back into the reduced first-order condition (2), we find that

$$(I - BA^\top C)B(l \circ u) = (I - BA^\top C)B(l \circ \ln(1 + x)). \quad (3)$$

We have thus managed to eliminate the Lagrange multipliers from the first-order condition.

2.3 A regression equation

Given a flow vector \hat{x} corresponding to demand b , we may now use (3) to motivate construction of a vector $y = (I - BA^\top C)B(l \circ \ln(1 + \hat{x}))$ and a matrix $w = (I - BA^\top C)B(l \circ z)$.

Doing this for each demand vector b , we may construct pairs (y_{bi}, w_{bi}) , where $b \in \mathcal{B}$ indexes the set of demand vectors and i indexes the elements of each vector y_b .

Adding mean zero noise terms ϵ_{bi} , we see that parameters β can be recovered from the regression

$$y_{bi} = w_{bi}\beta + \epsilon_{bi}. \quad (4)$$

We assume the noise terms to be independent of the variables in w_{bi} , but allow them to be heteroscedastic, which leads us to use robust standard errors when running regressions.

The computational complexity of the regression is independent of the number of route choice observations constituting the flow vector \hat{x} for each b , and only increases linearly with the size of the set of demand vectors \mathcal{B} , as the computationally most demanding task is obtaining the Moore-Penrose inverse C for each b .²

2.4 Routes are substitutes

The perturbed utility route choice model is formulated in terms of links, which we have seen is useful for estimation and avoids the need to enumerate the set of available routes. Proposition 1 shows that the model can (in principle, mathematically, not in practice) equivalently be formulated in terms of routes. This perspective allows some understanding to be gained of the model's behavior. The proposition shows that the equivalent model is a discrete choice model over the set of loop-free routes in which the routes are substitutes. An important driver of this result is that loops are ruled out by utility maximization.

Proposition 1. The perturbed utility route choice model is equivalent to a discrete choice model for the choice among all loop-free routes connecting origin to destination. The routes are substitutes, in the sense that if the utility of just one route is increased while the utility of all other routes are unaffected, then the choice probability weakly decreases for all other routes.

Proof of Proposition 1. Denote the set of all routes connecting origin to destination by Σ and a single route as a list of links $\sigma = \{e_{\sigma(1)}, e_{\sigma(2)}, \dots\}$. Any flow-conserving flow vector can be written as a sum of route flows. The utility function (1) can then be written in terms of vectors $p = \{p_\sigma, \sigma \in \Sigma\} \subseteq \mathbb{R}_+^{|\Sigma|}$ as

$$U(p) = \sum_{\sigma \in \Sigma} p_\sigma u_\sigma - G(p), \text{ where} \quad (5)$$

$$u_\sigma = \sum_{e \in \sigma} u_e, \quad G(p) = \sum_{e \in \mathcal{E}} l_e F\left(\sum_{\sigma \ni e} p_\sigma\right), \quad (6)$$

and where it is noted that we do not yet restrict the domain of G to probability vectors. The utility is strictly decreasing in each element of p , which means it is no loss of generality to restrict Σ to be

²We used the `IMqrqinv` function in Matlab (Ataei, 2014), which required less than 0.06 seconds per OD-combination. It is probably possible to utilize sparsity to speed this up.

finite, consisting only of routes with no loops. The function F is strictly convex by assumption and hence G is convex. In fact, it is strictly convex as shown by the following argument.

Assume $p^1 \neq p^2 \in \mathbb{R}_+^{|\Sigma|}$, then

$$\begin{aligned} G(\eta p^1 + (1-\eta)p^2) &= \sum_{e \in \mathcal{E}} l_e F\left(\eta \sum_{\sigma \ni e} p_\sigma^1 + (1-\eta) \sum_{\sigma \ni e} p_\sigma^2\right) \\ &\leq \eta \sum_{e \in \mathcal{E}} l_e F\left(\sum_{\sigma \ni e} p_\sigma^1\right) + (1-\eta) \sum_{e \in \mathcal{E}} l_e F\left(\sum_{\sigma \ni e} p_\sigma^2\right) \\ &= \eta G(p^1) + (1-\eta) G(p^2), \end{aligned}$$

where the inequality is strict for links e with $\sum_{\sigma \ni e} p_\sigma^1 \neq \sum_{\sigma \ni e} p_\sigma^2$. But such links exists, since $p^1 \neq p^2$ and hence G is strictly convex.

The convex conjugate of G restricted to the set of probability vectors is the indirect perturbed utility

$$U^*(u) = \sup_{p \in \Delta(\Sigma)} \{U(p)\} = \sup_{p \in \Delta(\Sigma)} \left\{ \sum_{\sigma \in \Sigma} p_\sigma u_\sigma - G(p) \right\}.$$

If G is supermodular, then its convex conjugate U^* is supermodular (e.g. [Feng et al., 2018](#), Lem. 1). So consider the mixed partial derivatives of the convex perturbation,

$$\frac{\partial^2 G(p)}{\partial p_{\sigma_1} \partial p_{\sigma_2}} = \sum_{e \in \mathcal{E}} l_e \frac{\partial F' \left(\sum_{\sigma \ni e} p_\sigma \right) 1_{\{e \in \sigma_1\}}}{\partial p_{\sigma_2}} = \sum_{e \in \mathcal{E}} F'' \left(\sum_{\sigma \ni e} p_\sigma \right) 1_{\{e \in \sigma_1 \cap \sigma_2\}},$$

to conclude they are either 0 for routes that do not overlap and otherwise negative. Hence the convex perturbation G is submodular and U^* is supermodular. Moreover, U^* satisfies the definition of a choice welfare function in [Feng et al. \(2018\)](#). Hence by [Feng et al. \(2018, Thm. 1\)](#), if U^* is differentiable then all routes are substitutes. But this holds by [Rockafellar \(1970, Thm. 26.3\)](#), since G is essentially strictly convex. \square

The proof of Proposition 1 shows that the perturbed utility model has an equivalent formulation as a perturbed utility model (5) for the choice among all loop-free routes connecting origin to destination. The convex perturbation G is a length-weighted sum across links of terms that are the convex function F applied to each link flow. The flow on link e is the sum of route choice probabilities for routes using that link, $\sum_{\sigma \ni e} p_\sigma$. The presence of such sums in the utility function generates a tendency to substitutability. In fact, if there was only one such term $F \left(\sum_{\sigma \ni e} p_\sigma \right)$, then routes using link e would be perfect substitutes.

3 Experimenting with the model

In this section we investigate the behavior of the model by solving the traveler’s problem, first on a small toy network, then on a large network for the Copenhagen metropolitan area.

3.1 A toy example

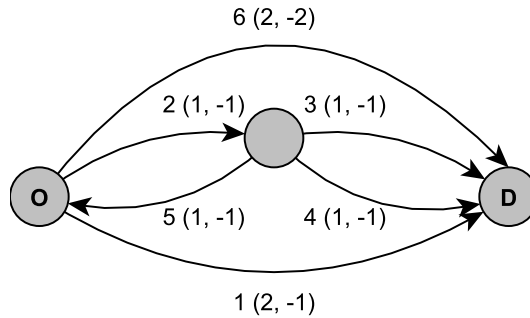


Figure 1: Toy network. Numbers in parentheses indicate length and unit cost, i.e. (l_e, u_e) .

Consider a toy network with six links and four loop-free routes from origin to destination, see Figure 1. One route uses link 1 with length $l_1 = 2$, which goes straight from the origin to the destination. Two routes share link 2 with length $l_2 = 1$ and then split into links 3 and 4 each also with length $l_3 = l_4 = 1$. The fourth route uses link 6 with length $l_6 = 2$ that also connects the origin with the destination directly. To test the ability of the perturbed utility model to handle the possibility that loops are possible, we add a link 5 that is equal to link 2 except it goes in the opposite direction, such that it is consistent with flow conservation to have flow looping on links 2 and 5. The unit link utility is $u_e = -1$ on all links, except for link 6 for which $u_6 = -2$. This causes three of the four direct routes to have the same total disutility, and the alternative using link 6 to be twice as costly.

The base case utility maximizing flows for the perturbed utility route choice (PURC) model are shown in Table 1. We have also included flows for a corresponding multinomial logit (MNL) model (McFadden, 1973) and a path-size logit (PSL) model (Ben-Akiva and Bierlaire, 1999)³. We note that the PURC model assigns zero flow on link 5, hence utility maximization causes the loop not to occur even though it is (physically) possible in the model. In contrast, the MNL and PSL models rely on generated choice sets for which we omitted paths with loops. We note also that the PURC model is able to assign zero flow to the costly link 6. In contrast, the MNL and PSL models both assign a positive flow since the route using link 6 is included in the choice set.

³Parameters for the multinomial logit model and the path-size logit model were calibrated against PURC flow. This was done on the base network, but due to equal utility on all used routes in PURC, we forced x_6 to be used by setting $u_6 = -1.25$. Disallowing loops for MNL and PSL, the parameters found to reduce the sum of square errors across the link flows were $\beta_u = 2.0$ and $\beta_{PS} = 1.1$.

	Link	l_e	u_e	PURC flow	MNL flow	PSL flow
Base	1	2	-1	0.424	0.331	0.404
	2	1	-1	0.576	0.663	0.589
	3	1	-1	0.288	0.331	0.294
	4	1	-1	0.288	0.331	0.294
	5	1	-1	0	0 ⁴	0 ⁴
	6	2	-2	0	0.006	0.007
Increase unit cost on link 4 (rel. to base)	1	2	-1	0.445 (1.047)	0.352 (1.064)	0.427 (1.056)
	2	1	-1	0.555 (0.965)	0.641 (0.967)	0.566 (0.961)
	3	1	-1	0.342 (1.187)	0.352 (1.064)	0.311 (1.056)
	4	1	-1.1	0.214 (0.743)	0.289 (0.871)	0.255 (0.865)
	5	1	-1	0 -	0 ⁴ -	0 ⁴ -
	6	2	-1	0 -	0.006 (1.064)	0.008 (1.056)
Move node at the end of link 2 (rel. to base)	1	2	-1	0.381 (0.897)	0.331 (1)	0.364 (0.902)
	2	0.5	-1	0.619 (1.076)	0.663 (1)	0.629 (1.069)
	3	1.5	-1	0.310 (1.076)	0.331 (1)	0.315 (1.069)
	4	1.5	-1	0.310 (1.076)	0.331 (1)	0.315 (1.069)
	5	0.5	-1	0 -	0 ⁴ -	0 ⁴ -
	6	2	-2	0 -	0.006 (1)	0.007 (0.902)

Table 1: Utility maximizing flows in toy network.

We consider two experiments. In the first, we increase the unit cost on link 4 by 0.1. In all three models, this leads to a decrease in the flow on the route using link 4. In the PURC model, the flow on the route using link 3 increases more in relative terms than the flow on link 1. Thus, the IIA property does not hold in the PURC model: the routes using links 3 and 4 are closer substitutes with each other than with the route using link 1. This is a desirable property, which occurs since the two close routes share link 2. In contrast, in the MNL and PSL models, the flow on the routes using links 1, 3 and 6 increase by the same proportion, in accordance with the IIA property.

In the second experiment, we reduce the length of link 2 and 5 by 0.5 and increase the lengths of links 3 and 4 by the same amount. This makes the routes using link 2 more dissimilar and hence attracts more flow to them in the PURC model. The limiting cases of this kind of change are as desired: the utility maximizing flows split evenly on the three routes if link 2 is reduced to zero length, and the utility maximizing flows split fifty-fifty if the length of link 2 is increased to 2. In other words, as the two routes overlap less, they function as more independent routes. In contrast, the change in link lengths leads to no change in flows in the MNL model. The PSL model reacts similarly to the PURC model in this case.

3.2 Illustration using the Copenhagen metropolitan area road network

We proceed to illustrate how the perturbed utility model behaves on a large network. We use a network, shown in Figure 2, for the Copenhagen metropolitan area comprising 30,773 links and

⁴Zero flow purely a consequence of the choice set generation method.

12,876 nodes (Kjems and Paag, 2019).

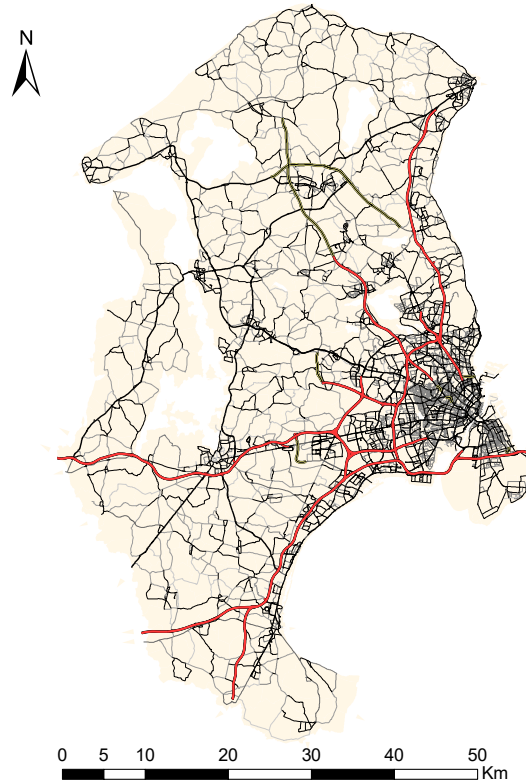


Figure 2: Network of the Copenhagen metropolitan area

Figure 3 shows the model's prediction for a trip from the airport (located South-East on the figure) to the Technical University of Denmark (North). For the example we specified the link utility as a parameter β multiplied by travel time and used different values of β . We solved the traveler's problem using MatLab (MATLAB, 2010) with the `fmincon` command using an Interior Point Algorithm (Byrd et al., 1999; Waltz et al., 2006) approach for constrained optimization.

The first thing to notice is that most links in the network are inactive having zero predicted flow. As in Proposition 1, the active links and the predicted flows can be translated into a set of active routes with corresponding route choice probabilities.

The model predicts two clear main alternatives. One using the Western motorway bypass across Kalvebod bridge (Kalvebodbroen), and a cluster of alternatives going through the city center. When β is numerically small, the number of active routes is high even if most of the network remains unused. Link usage approaches the shortest (fastest) path as β increases numerically. Especially use of the cluster of alternatives through the city center is reduced when β becomes numerically larger.

Figure 4 shows the change in predicted flows that follows an increase in the travel time on Kalvebodbroen in the southern part of the map by two minutes. This change increases the cost on

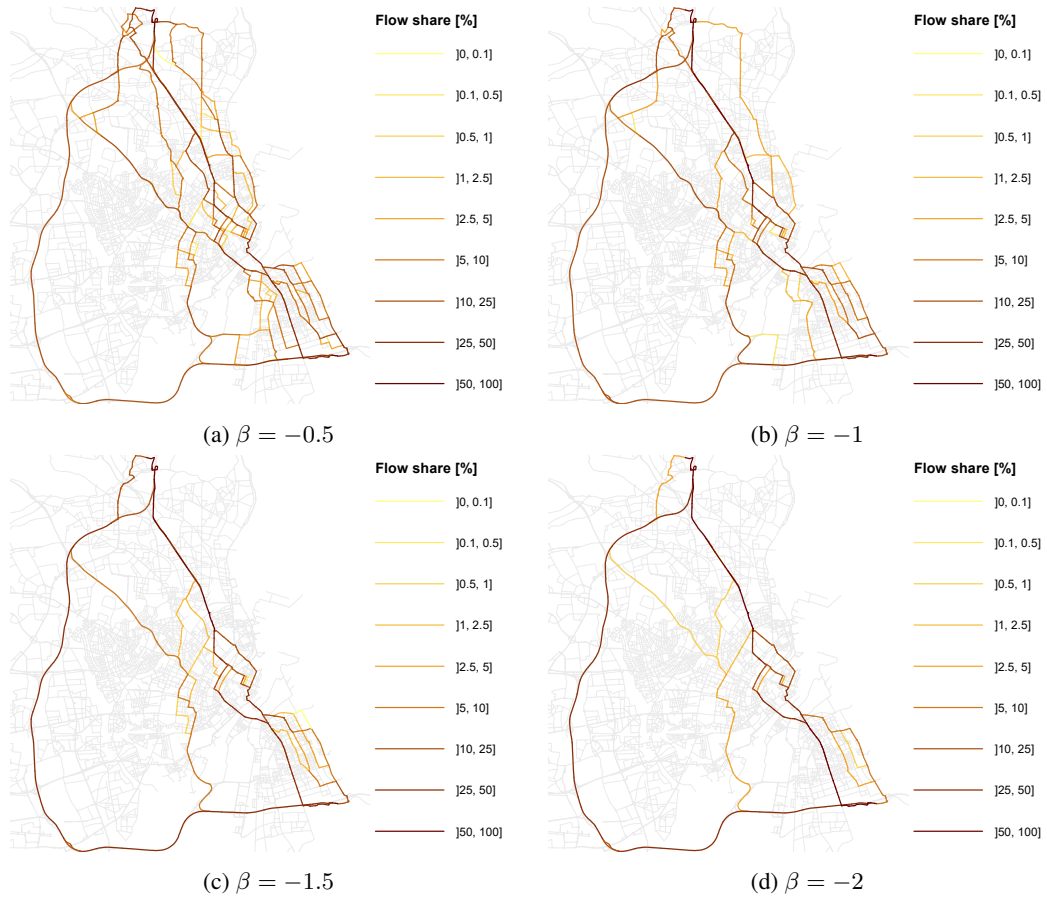


Figure 3: Flow shares from Copenhagen Airport to Technical University of Denmark for different values of β

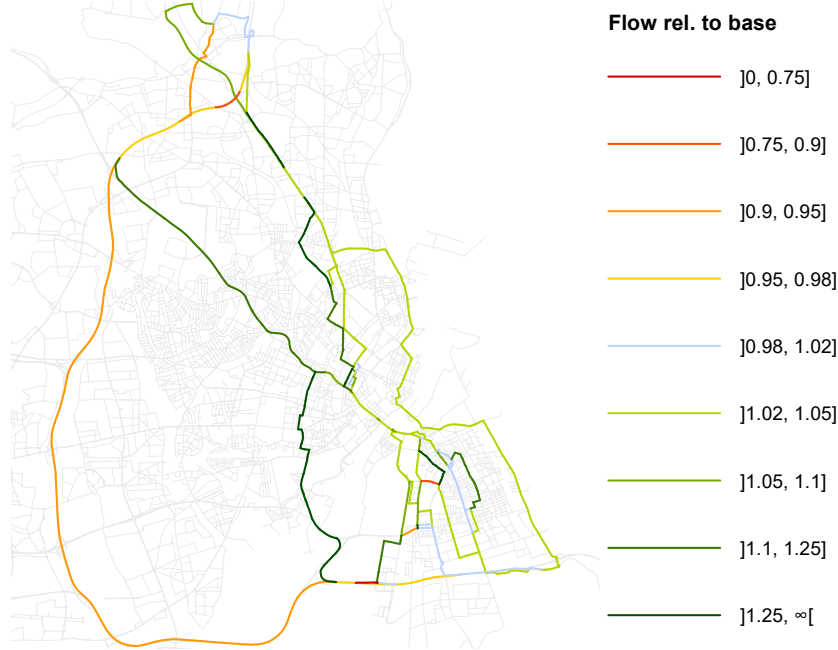


Figure 4: Substitution patterns for trips between Copenhagen Airport and Technical University of Denmark using parameters estimated in model C below and increasing travel time on Kalvebodbroen by 2 minutes

all routes that use Kalvebodbroen and consequently flow shifts to alternative routes. Routes that share links with routes that use Kalvebodbroen are closer substitutes, which confirms the theoretical expectation.

4 Testing the estimator on simulated data for Copenhagen

In this section, we test the ability of the estimator to recover a known true parameter from data simulated from the model.

We have pre-selected 22 nodes that are used as origins/destinations. Sampling from these, we have generated a number of datasets of using a different number of origin-destination combinations (1, 5, 20 and 100) and different values of a parameter for travel time ($\beta \in \{-3, -2.5, \dots, -0.5\}$). For each origin-destination and β , we have solved the traveler's problem and sampled a number of route choices consistent with the predicted link flows. This mimics actual data collection but in a case where the true model is known. We have created datasets sampling, respectively, 25, 100, 250 and 1000 route choices for each origin-destination.

Altogether, we have created $4 \times 4 \times 6 = 96$ datasets. For each dataset, treating it as if it was real data, we have computed a flow vector x for each origin-destination. We have then transformed the

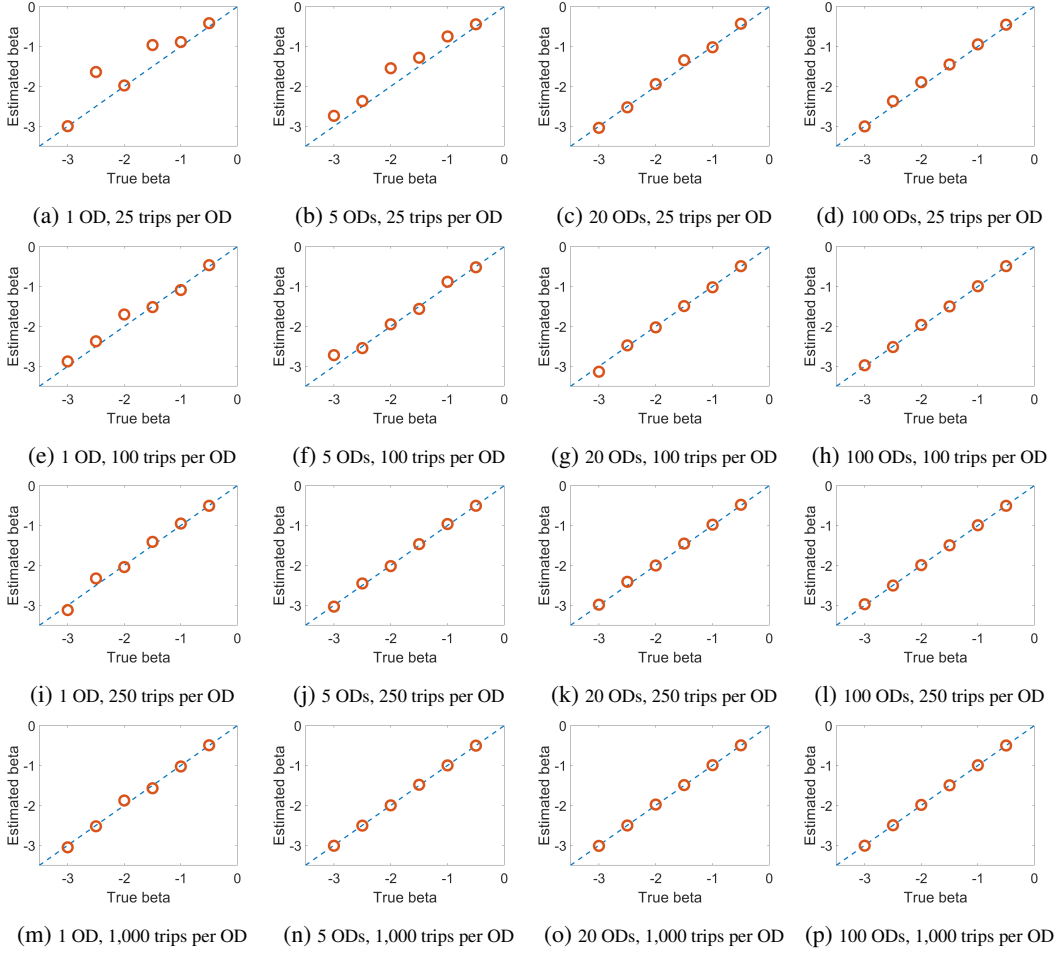


Figure 5: Parameter estimates against the true parameters for different combinations number of trips per origin-destination relation and number of origin-destination relations.

data as described in Section 2.3 and estimated β using OLS.

We have used all observations for all links with positive flow without applying any truncation. This might have led to bias as the function $\ln(1+x)$ that transforms the flows is nonlinear and the flows are estimated with considerable noise. As the results in Figure 5 show, we find no visible bias when the number of origin-destinations and the number of route choices are sufficiently large. It seems plausible that the reason we do not find any noticeable bias is that the logarithm $\ln(1+x)$ is close to linear for small values of x .

Altogether, the results are encouraging. We find that it is possible to recover the true parameter from a sample of routes with good precision. The estimates seem to be biased toward zero, when the dataset is small, but the bias is negligible at moderate dataset sizes.

Figure 6 shows cumulative distributions of some summary statistics of the simulated flows un-

derlying the simulation. Panel (a) shows how the number of active links increases as the travel time parameter β approaches zero and the influence of travel time diminishes. Panel (b) shows that, as expected, a numerically smaller travel time parameter increases the average predicted travel time.

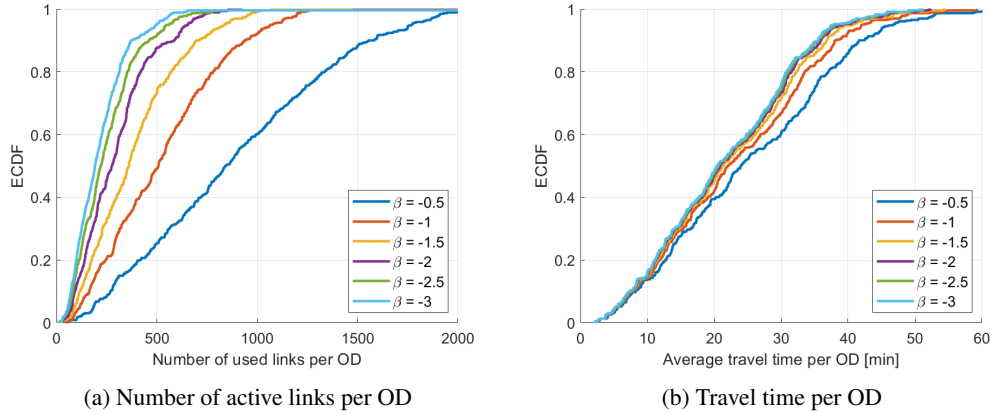


Figure 6: Cumulative distribution for simulated route choices in Figure 3

5 Empirical application

5.1 Estimation

Our empirical application uses an estimation dataset comprising 8,046 active OD-combinations and 1,337,096 trips. It is based on GPS vehicle trajectory data for the Copenhagen metropolitan area. The data processing is described in Appendix A.

To explain the observed route choices, we use average observed travel time per link⁵, the number of outlinks and dummies for road type. Table 2 reports estimation results for three different model specifications. Numbers in parentheses are robust standard errors. As can be seen, all parameters are very precisely estimated.

Model A comprises just a parameter for travel time, which is seen to be estimated with extreme precision. Comparison with the simulations in Figure 3 suggests the range is quite reasonable.

In model B, we extend with a constant for each link having at least two outlinks. This penalizes links that lead into intersections. The travel time parameter is reduced in absolute value as could be expected. The adjusted R-square increases quite a bit, indicating preference for model B over model A.

In model C, we interact the travel time variable with link type dummies to estimate travel time parameters that are specific to each link type. The sign and relative sizes of these parameters make

⁵A total of 9,464,883 trips were used for determining the empirical average link travel times.

	Model A	Model B	Model C
Constant _{Outlinks\geq2}	–	-0.03428 (0.00030)	-0.01546 (0.00030)
Travel time [min.]	-0.74642 (0.00171)	-0.63773 (0.00225)	–
Travel time [min.]:			
<i>Motorways</i>	–	–	-0.35011 (0.00342)
<i>Motorway ramps</i>	–	–	-0.55419 (0.00437)
<i>Motor traffic roads</i>	–	–	-0.56233 (0.00464)
<i>Other national roads</i>	–	–	-0.59969 (0.00297)
<i>Urban roads</i>	–	–	-0.56917 (0.00219)
<i>Rural roads</i>	–	–	-0.77783 (0.00308)
<i>Smaller roads</i>	–	–	-0.53003 (0.01101)
<i>Other ramps</i>	–	–	-0.44558 (0.00448)
Adjusted R^2	0.36288	0.36855	0.40880

Table 2: Estimation results

intuitive sense. The adjusted R-square increases again quite a bit, indicating preference for model C over model B.

5.2 Validation

We go on to validate the prediction of model C against our data. For each OD-combination in the data, we compute the predicted flow vector using the estimated parameters. We compare this prediction to the estimation dataset to ascertain the ability of the model to reproduce these data. The main text shows validation results using the full sample. We have a large dataset and a model with few parameters, so results are not likely to be very vulnerable to over-fitting. However, we test out of sample predictions in Appendix B, where we have split the data at random by OD-combination into two equal sized datasets. We have estimated the model for each sample split and apply each set of estimated parameters to make predictions for the other half of the sample. The parameter estimates for the two sample splits found in Appendix B are very similar and the out of sample prediction test did not reveal any issues.

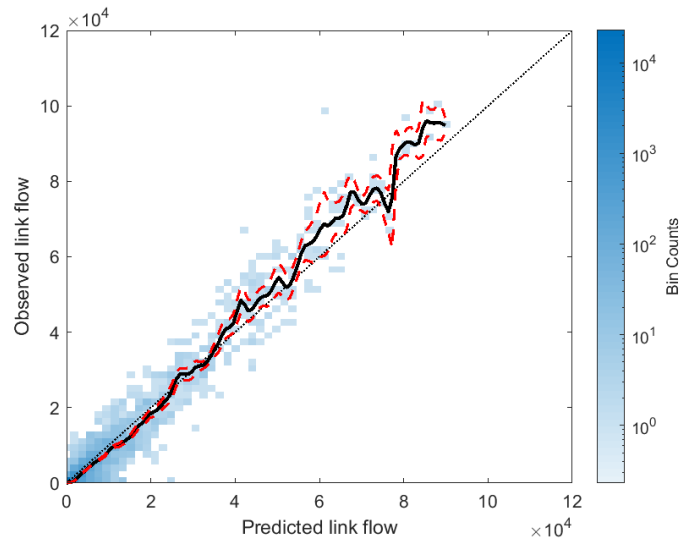


Figure 7: Observed vs predicted total link flows when summing across all OD pairs.

Figure 7 shows the main validation result, comparing observed link flows to the predicted. We observe that predictions are generally close to the 45° line. A nonparametric fit with 95% confidence bands suggests some systematic deviations but the general conclusion is that the model is well able to meaningfully predict the observed flows. We do find the fit to be quite satisfactory, as we have employed no calibration whatsoever - the predictions are driven solely by the 9 estimated parameters in Table 2.

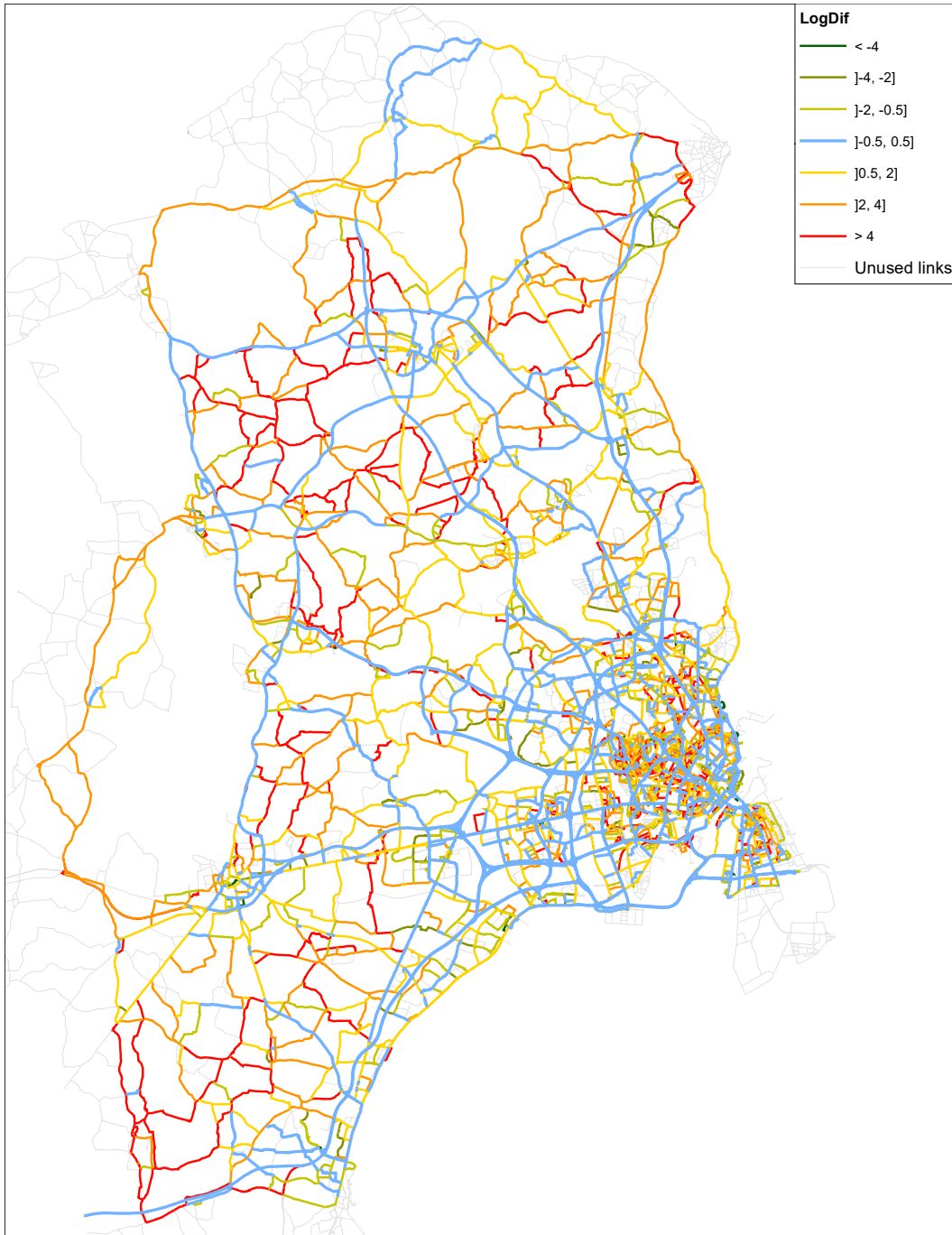


Figure 8: Regional difference map. Differences given as $\ln(q^{\text{predicted}} + 1) - \ln(q^{\text{observed}} + 1)$.

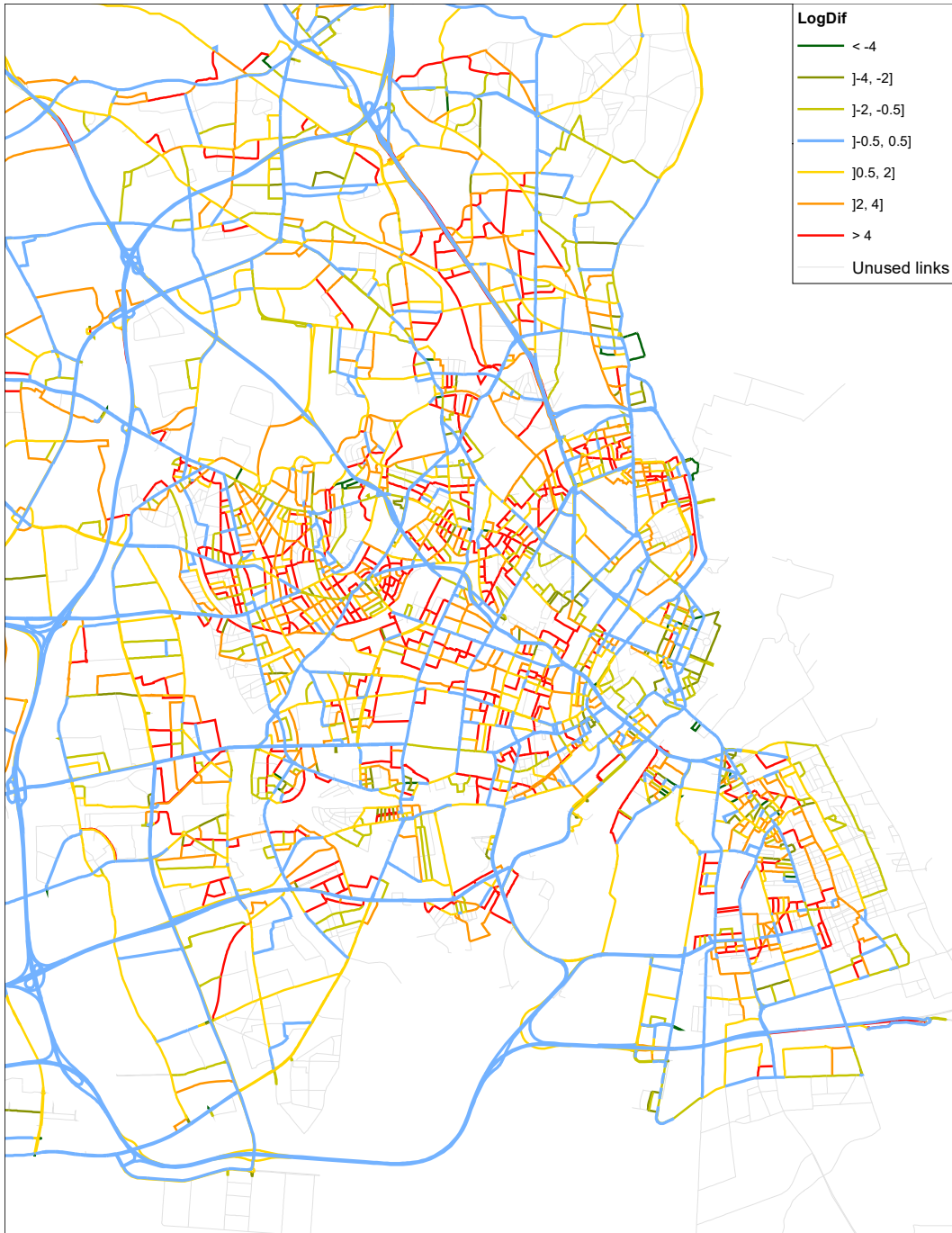


Figure 9: City-wide difference map. Differences given as $\ln(q^{\text{predicted}} + 1) - \ln(q^{\text{observed}} + 1)$.

Figures 8 and 9 visualize the comparison between predicted and observed flows on a map of the network. Blue links are well predicted, the model predicts too much traffic on red links and too

little on green links compared to observed. We observe that the main road network is generally blue on the figure, while red links tend to be minor roads. We find this result to be quite satisfactory, indicating that the estimated model is able to predict a large share of the variation in observed link flows.

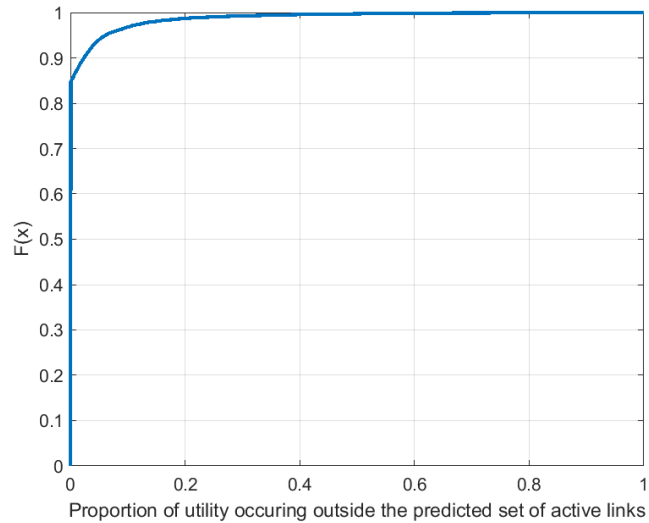


Figure 10: Cumulative distribution function of proportion of utility of observed trips outside the predicted set of active links.

An issue that has troubled modeling approaches that rely on a predefined consideration set is that the observed routes may not be covered by the consideration set. In contrast, the perturbed route choice model takes all potential routes into account and predicts a set of active links. It is then relevant how well these predicted sets of active links, one set for each OD-combination, cover the chosen routes. Figure 10 shows the cumulative distribution of the proportion of utility of chosen routes that is outside the predicted set of active links. Hence a value of zero is perfect and small values are good. We find that about 85% of observed trips are completely inside the predicted set of active links and almost all observed trips have less than 20% of utility outside the predicted set of active links.

6 Conclusion

This paper has opened the door to a new way to model route choice. The perturbed utility route choice model can be estimated using just linear regression, it is straightforward to use for assignment, and it produces reasonable substitution patterns. We have estimated and applied the model to a large dataset covering the Copenhagen metropolitan area and found that the model is well able to

predict much of the variation in observed flows, thereby demonstrating the feasibility of applying the model in practice.

We do not claim to have found the perfect model. But we do hope to have convinced readers that the perturbed utility model is a worthwhile alternative to previous existing approaches. There are many ways to go forward from here.

We have ignored sampling error in the observation of flows. Our simulations suggest this is not a problem when the number of observations is sufficiently large. Further work might incorporate weighting to reflect the number of observations used for estimating flows. It would also be of interest to be able to estimate the model with individual level data, perhaps adapting the iteratively reweighted least squares algorithm of [Nielsen et al. \(2021\)](#).

We have worked with a static and deterministic network. It might be possible to adapt the perturbed utility route choice model to more complex settings.

An interesting question is the shape of the perturbation function. There is considerable freedom within the requirement imposed on F and there are many other options in addition to the one we have chosen. The effect of using other perturbation functions remains an open issue, theoretically as well as empirically. Another direction that could be explored is to add cross-link interactions as a means to control the substitution patterns of the model. One way to go might be along the lines of the nested recursive logit model ([Mai et al., 2015a](#)).

Finally, we note that our model seems to fit nicely into the equilibrium assignment in [Oyama et al. \(2020\)](#). This research direction also seems appealing.

A Data processing

The raw data comprises 472,801,802 GPS points corresponding to 9,464,883 trips. The data covers a 3 month period from June 1 2019 to August 31 2019.

A.1 Map-matching

The data has been map-matched to the network using a branch-and-bound based algorithm proposed in [Nielsen et al. \(2007\)](#). This led to 8,039,296 map-matched trips. Some trips were only partially map-matched, we retain 5,320,215 trips for which the whole trajectory could be matched successfully.

A.2 Trimming trips

To ensure that we have sufficiently many trips with origin-destination combination in common we have devised an algorithm to trim the start of trips such that they begin in a smaller set of nodes in the network. We have used the same algorithm to trim the end of trips to arrive at a smaller set of common destination nodes.

The algorithm is based on a sample of trips \mathcal{T} , where each trip $t \in \mathcal{T}$ is the sequence of nodes visited $t = (v_1^t, \dots, v_{n_t}^t)$. Denote by \mathcal{T}_v the set of trips that passes through node v , and let k_*^t denote the first occurrence of a selected node for trip $t \in \mathcal{T}$. The algorithm iteratively trims trips in a given set of trips until the number of unique origin nodes is reduced to a prespecified number N_O . It comprises the following steps.

1. Initialise the set of chosen origin nodes, \mathcal{V}_O , as the empty set, $\mathcal{V}_O = \emptyset$, and set $k_*^t = n^t$ for all $t \in \mathcal{T}$.
2. Calculate the trip score $S_{v_k^t}^t$ for every node v_k^t , $k = 1, \dots, n_t$ of every trip $t \in \mathcal{T}$ as the number of remaining nodes of that trip: $S_{v_k^t}^t \leftarrow k_*^t - k$.
3. Calculate the score of each node $v \in \mathcal{V}$ as the sum of the trip scores across trips: $S_v \leftarrow \sum_{t \in \mathcal{T}_v} S_v^t$.
4. Add the highest scoring node $v^* = \arg \max_{v \in \mathcal{V}} S_v$ to the set of selected nodes, i.e. $\mathcal{V}_O \leftarrow \mathcal{V}_O \cup v^*$.
5. For each trip $t \in \mathcal{T}$ for which $v^* \in t$, (potentially) update the first occurrence of a selected node by $k_*^t \leftarrow \min k : v_k^t \in \mathcal{V}_O$.
6. Repeat steps 2-5 until $|\mathcal{V}_O| = N_O$.
7. Return \mathcal{V}_O .

We have run the algorithm to trim the data to 100 origins and 100 destinations to obtain the sets of valid origins and destinations, \mathcal{V}_O and \mathcal{V}_D . Figure 11 shows the resulting origins and destinations.

This allows trimming each trip $t \in \mathcal{T}$ so that it begins the first time it visits a node $v \in \mathcal{V}_O$, and ends the last time it visits a node $v \in \mathcal{V}_D$. A trip has to visit its first valid origin node before reaching its last valid destination node, otherwise the trip is discarded. Likewise, trips that do not pass through a valid origin node and a valid destination node are also discarded. We retain 1,680,667 trimmed trips that visit their first valid origin node before reaching their final valid destination node.

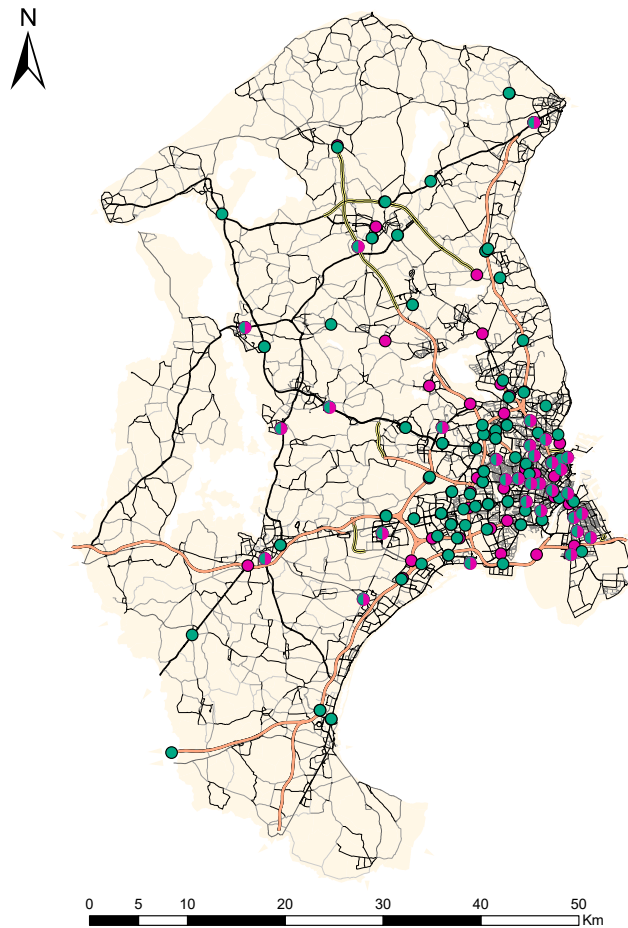


Figure 11: "Pseudo" origin (green) and destination (red) nodes.

A.3 Deleting non-sensical observations

The 1,680,667 observations with valid OD-sections covered a total of 9,284 different OD-combinations. We discarded 1,238 OD-combinations for which all trips used the same links, 187,790 trips were

thus discarded.

Some observed trips were non-sensical, perhaps due to detours for intermediate trip purposes. To identify such trips, we ran a prediction of the model for each OD-combination, using a travel time parameter of -0.3 , which is much lower than the estimated parameter in model A. The set of active links predicted as active with that single parameter is then quite large and likely to comprise most reasonable routes.

We have then used the selection criterion that observed routes should have at least 95% of their utility⁶ inside the active set. This criterion led us to discard 155,781 trips.

In the end, we arrived at an estimation dataset comprising 8,046 active OD-combinations and 1,337,096 trips.

B Estimation results for sample splits

In order to perform out of sample estimations, the 8,046 OD combinations were randomly split in two halves. Both contain 4,023 OD combinations and the number of trips is about the same; 668,330 trips in sample split 1 and 668,766 trips in sample split 2.

Tables 3 and 4 present the estimation results for the two sample splits. The parameter estimates are very similar.

	Model A	Model B	Model C
Constant _{Outlinks\geq2}	–	-0.03423 (0.00043)	-0.01512 (0.00044)
Travel time [min.]	-0.75163 (0.00246)	-0.64228 (0.00325)	–
Travel time [min.]:			
<i>Motorways</i>	–	–	-0.35801 (0.00492)
<i>Motorway ramps</i>	–	–	-0.55902 (0.00621)
<i>Motor traffic roads</i>	–	–	-0.58478 (0.00638)
<i>Other national roads</i>	–	–	-0.60969 (0.00428)
<i>Urban roads</i>	–	–	-0.57789 (0.00322)
<i>Rural roads</i>	–	–	-0.77801 (0.00438)
<i>Smaller roads</i>	–	–	-0.54239 (0.01211)
<i>Other ramps</i>	–	–	-0.46494 (0.00626)
Adjusted R^2	0.36394	0.36956	0.40945

Table 3: Estimation results for sample split 1

⁶In this case, simply travel time

	Model A	Model B	Model C
Constant _{Outlinks\geq2}	–	-0.03428 (0.00030)	-0.01577 (0.00042)
Travel time [min.]	-0.74131 (0.00238)	-0.63332 (0.00312)	–
Travel time [min.]:			
<i>Motorways</i>	–	–	-0.34169 (0.00475)
<i>Motorway ramps</i>	–	–	-0.54917 (0.00614)
<i>Motor traffic roads</i>	–	–	-0.53683 (0.00676)
<i>Other national roads</i>	–	–	0.58954 (0.00410)
<i>Urban roads</i>	–	–	-0.56045 (0.00297)
<i>Rural roads</i>	–	–	-0.77761 (0.00435)
<i>Smaller roads</i>	–	–	-0.51859 (0.01855)
<i>Other ramps</i>	–	–	-0.42436 (0.00642)
Adjusted R^2	0.36185	0.36755	0.40832

Table 4: Estimation results for sample split 2

We have carried out two set of out of sample predictions with the models, using parameters estimated on one sample split in the prediction for the other sample split. Figures 12-13 show scatter plots of observed vs. predicted link flows.

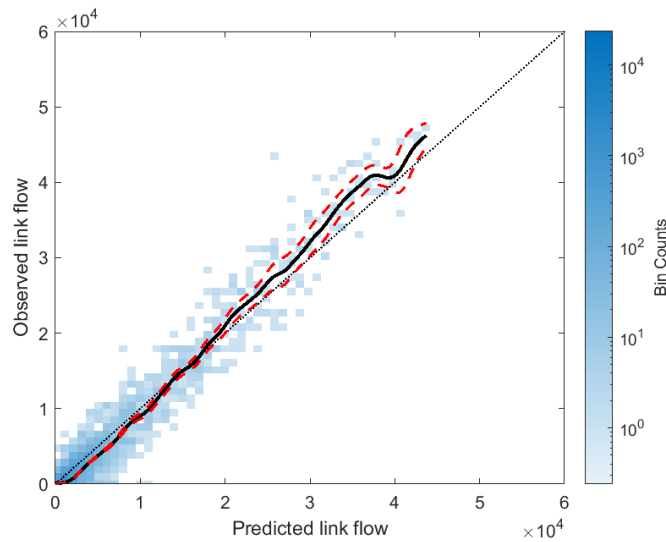


Figure 12: Observed vs predicted total link flows when summing across all OD pairs (sample split 2 using parameters estimated on sample split 1).

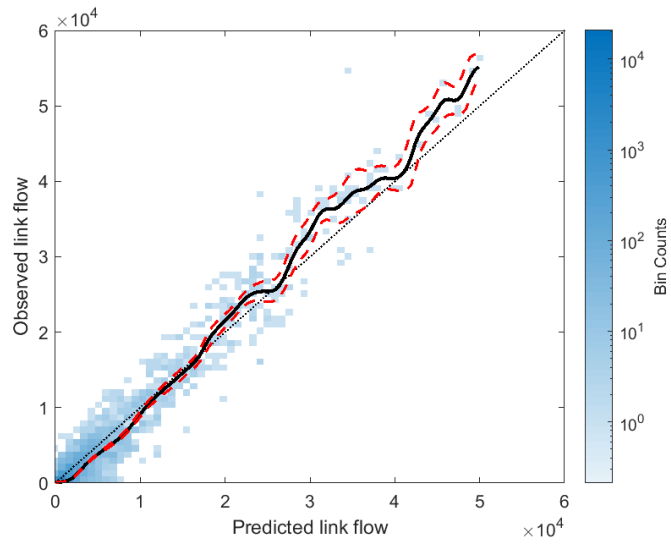


Figure 13: Observed vs predicted total link flows when summing across all OD pairs (sample split 1 using parameters estimated on sample split 2).

References

- ALLEN, R. AND J. REHBECK (2019): “Identification With Additively Separable Heterogeneity,” *Econometrica*, 87, 1021–1054.
- ATAEI, A. (2014): “Improved Qrginv Algorithm for Computing Moore-Penrose Inverse Matrices,” *ISRN Applied Mathematics*, 2014, 1–5.
- BAILLON, J. B. AND R. COMINETTI (2008): “Markovian traffic equilibrium,” *Mathematical Programming*, 111, 33–56.
- BELL, M. G. (1995): “Alternatives to Dial’s logit assignment algorithm,” *Transportation Research Part B*, 29, 287–295.
- BEN-AKIVA, M. AND M. BIERLAIRE (1999): *Discrete Choice Methods and their Applications to Short Term Travel Decisions*, Boston, MA: Springer US, 5–33.
- BYRD, R. H., M. E. HRIBAR, AND J. NOCEDAL (1999): “An Interior Point Algorithm for Large-Scale Nonlinear Programming,” *SIAM Journal on Optimization*, 9, 877–900.
- DIAL, R. B. (1971): “A probabilistic multipath traffic assignment algorithm which obviates path enumeration,” *Transportation Research*, 5, 83–111.
- FENG, G., X. LI, AND Z. WANG (2018): “On substitutability and complementarity in discrete choice models,” *Operations Research Letters*, 46, 141–146.
- FOSGERAU, M., E. FREJINGER, AND A. KARLSTROM (2013): “A link based network route choice model with unrestricted choice set,” *Transportation Research Part B: Methodological*, 56, 70–80.
- FOSGERAU, M. AND D. L. MCFADDEN (2012): “A theory of the perturbed consumer with general budgets,” *NBER Working Paper*, 1–27.
- FUDENBERG, D., R. IJIMA, AND T. STRZALECKI (2015): “Stochastic Choice and Revealed Perturbed Utility,” *Econometrica*, 83, 2371–2409.
- HOFBAUER, J. AND W. H. SANDHOLM (2002): “On the global convergence of stochastic fictitious play,” *Econometrica*, 70, 2265–2294.
- KJEMS, S. AND H. PAAG (2019): “COMPASS: Ny trafikmodel for hovedstadsområdet,” *Proceedings from the Annual Transport Conference at Aalborg University*.
- MAI, T., M. FOSGERAU, AND E. FREJINGER (2015a): “A nested recursive logit model for route choice analysis,” *Transportation Research Part B: Methodological*, 75, 100–112.

- MAI, T., E. FREJINGER, AND F. BASTIN (2015b): “A Dynamic Programming Approach for Quickly Estimating Large Scale MEV Models,” *Transportation Research Part B: Methodological*.
- MATLAB (2010): *MATLAB:2010*, Natick, Massachusetts: The MathWorks Inc.
- McFADDEN, D. (1981): “Econometric Models of Probabilistic Choice,” in *Structural Analysis of Discrete Data with Econometric Applications*, ed. by C. Manski and D. McFadden, Cambridge, MA, USA: MIT Press, 198–272.
- McFADDEN, D. L. (1973): “Conditional logit analysis of qualitative choice behavior,” in *Frontiers in Econometrics*, New York: Academic Press, 105–142.
- NIELSEN, N., M. FOSGERAU, AND D. KRISTENSEN (2021): “Estimation of perturbed utility models using demand inversion,” *Working Paper*.
- NIELSEN, O., C. WÜRTZ, AND R. JØRGENSEN (2007): “Improved map-matching algorithms for GPS-data - - Methodology and test on data from The AKTA roadpricing experiment in Copenhagen.” European ITS Conference ; Conference date: 18-06-2007 Through 20-06-2007.
- OYAMA, Y., Y. HARA, AND T. AKAMATSU (2020): “Markovian Traffic Equilibrium Assignment based on Network Generalized Extreme Value Model,” *arXiv*.
- PRATO, C. G. (2009): “Route choice modeling: Past, present and future research directions,” *Journal of Choice Modelling*, 2, 65–100.
- ROCKAFELLAR, R. T. (1970): *Convex Analysis*, Princeton, N.J.: Princeton University Press.
- SHEN, W., H. M. ZHANG, AND T. AKAMATSU (1996): “Cyclic flows, Markov process and stochastic traffic assignment,” *Transportation Research Record*, 30, 1–34.
- WALTZ, R. A., J. L. MORALES, J. NOCEDAL, AND D. ORBAN (2006): “An interior algorithm for nonlinear optimization that combines line search and trust region steps,” *Mathematical Programming*, 107, 391–408.
- WATLING, D. P., T. K. RASMUSSEN, C. G. PRATO, AND O. A. NIELSEN (2015): “Stochastic user equilibrium with equilibrated choice sets: Part I - Model formulations under alternative distributions and restrictions,” *Transportation Research Part B: Methodological*, 77, 166–181.
- (2018): “Stochastic user equilibrium with a bounded choice model,” *Transportation Research Part B: Methodological*, 114, 254–280.